Technical Note : A universal method for measuring the thickness of microscopic calcite crystals, based on Bidirectional Circular Polarization

Luc Beaufort[1], Yves Gally[1], Baptiste Suchéras-Marx[1], Patrick Ferrand[2], Julien Duboisset[2]

[1]Aix Marseille Univ, CNRS, IRD, INRAE, Coll. France, CEREGE, Aix-en-Provence, France
[2] Aix Marseille Univ, CNRS, Centrale Marseille, Institut Fresnel, Marseille, France

Correspondence to: Luc Beaufort (beaufort@cerege.fr)

Abstract. The coccoliths are major contributors to the particulate inorganic carbon in the ocean that is a key part of the carbon cycle. The coccoliths are few microns in length and weigh few picograms. Their birefringence characteristics in polarized optical microscopy has been used to estimate their mass. This method is rapid and precise because camera sensors produce excellent measurement of light. However, current method is limited because it requires a precise and replicable set up and calibration of the light in the optical apparatus. Precisely, the light intensity, the diaphragm opening, the position of the condenser, and the exposure time of the camera have to be strictly identical during the calibration and the analysis of calcite crystal. Here we present a new method that is universal in the sense that the thickness estimations are independent from a calibration but results from a simple equation. It can be used with different cameras and microscope brand. Moreover, the light intensity used in the microscope does not have to be strictly and precisely controlled. This method permits to measure crystal thickness up to 1.7 µm. It is based on the use of one left circular polarizer and one right circular polarizer with a monochromatic light source using the following equation:

$$d = \frac{\lambda}{\pi \Delta n} arctan\left(\sqrt{\frac{I_{LR}}{I_{LL}}}\right)$$

where d is the thickness, λ the wavelength of the light used, Δn the birefringence, I_{LR} and I_{LL} are the light intensity measured with a right and a left circular polarizer. Because of the alternative and rotative motion of the quarter-wave plate of the circular polarizer, we coined the name of this method 'Bidirectional Circular Polarization' (BCP).

1 Introduction

Coccolithophores are abundant oceanic single cell algae that produce calcite plate called coccoliths. The coccoliths are major contributors to the particulate inorganic carbon (i.e., PIC) in the ocean that is a key part of the carbon cycle. The coccoliths are so minute (few microns in length) and light (few picograms) that they can be weighed individually only with extreme labor and expensive apparatus (Hassenkam et al., 2011;Beuvier et al., 2019). Alternatively, the birefringence characteristic of coccolith in polarized optical microscopy has been used to estimate their mass (Beaufort, 2005;Beaufort et al., 2014;Bollmann,

2014;Fuertes et al., 2014). This method is rapid and precise. The camera sensor produces excellent measurement of light. The camera sensor measures the light that had come through the polarizers and a calcite crystals to convert into a thickness value. The estimation made by this method has been recently positively evaluated by the independent measurements made by X-ray tomography at the European Synchrotron Radiation Facility (ESRF) (Beuvier et al., 2019). One of its limitations is that it needs a precise calibration of the lightness of the microscope. The light intensity, the diaphragm opening, the position of the condenser, and the exposure time of the camera, have to be strictly identical between the calibration and the analysis of the calcite crystal. Slight change on one of those parameters have important consequence on the results. Another limitation is that the measured light intensity is not linearly proportional to the thickness but follow a sigmoid (Beaufort et al., 2014;Bollmann, 2014) making difficult to estimate the thickness precisely at the two ends of the calibration. The use of standard polychromatic « white » light induce a small imprecision, because the temperature of light that depends on the microscope – some have a bluish light other have it more yellowish – will change slightly the result if not calibrated. There is a theoretical limit of the thickness estimation to about 1.56 µm when using a black and white camera. The estimation of calcite particles thicker than 1.56 µm needs to be done with a color camera with several calibration equations (Beaufort et al., 2014;González-Lemos et al., 2018). Here we propose a new method that solve those problems: the estimations are not the results of a calibration, they can be applied to crystals as thick as 1.7 µm, and are not dependent on the precise tuning of the light of the microscope.

2 Principles

The representation of the polarized light is based on Jones's calculus (Jones, 1941). The microscope is composed of two circular polarizers – one left oriented and the other right oriented – used alternatively and one circular analyzer.

2.1 Jones Matrices

For an anisotropic material having its ordinary neutral axis horizontal, Jones matrix is given by

$$\boldsymbol{W}_0 = T \begin{bmatrix} 1 & 0 \\ 0 & (1-\eta)e^{i\phi} \end{bmatrix}$$

where T is the (complex) transmission coefficient, η is the diattenuation, and ϕ is the retardation, with $\phi = \frac{2\pi}{\lambda}\Delta nd$ (where λ is the wavelength, Δn is the birefringence, d is the thickness).

If the neutral axis is rotated by an angle θ, the Jones matrix becomes

$$\boldsymbol{W}_\theta = \boldsymbol{R}(-\theta).\boldsymbol{W}_0.\boldsymbol{R}(\theta)$$

where $\boldsymbol{R}(\theta)$ is the rotation matrix

$$\boldsymbol{R}(\theta) = \begin{bmatrix} cos\theta & sin\theta \\ -sin\theta & cos\theta \end{bmatrix}$$

2.2 Proposed measurement scheme

Assuming that $\eta = 0$ (no diattenuation), the input field is left-circularly polarized

$$P_L = \frac{1}{\sqrt{2}}\begin{bmatrix} 1 \\ i \end{bmatrix}$$

60 and the polarization analysis involved either a left circular polarizer made of a quarter-wave plate at 45° followed by a horizontal polarizer

$$A_L = \begin{bmatrix} 1+i & 1-i \\ 0 & 0 \end{bmatrix}$$

or a right circular polarizer (made of a quarter-wave plate at -45° followed by a horizontal polarizer)

65

$$A_R = \begin{bmatrix} 1+i & -1+i \\ 0 & 0 \end{bmatrix}$$

so that the measured intensities writes

$$I_{LL} = |A_L.W_\theta.p_L|^2 = |T|^2 sin^2\left(\frac{\phi}{2}\right)$$

and

$$I_{LR} = |A_R.W_\theta.p_L|^2 = |T|^2 cos^2\left(\frac{\phi}{2}\right)$$

70

2.3 Retrieving thickness

One can see that I_{LL} and I_{LR} do not depend on the orientation θ of the neutral axes.
Moreover, the ratio

$$\frac{I_{LL}}{I_{LR}} = tan^2\left(\frac{\phi}{2}\right) = tan^2\left(\frac{\pi}{\lambda}\Delta nd\right), \tag{1}$$

75

does not depend on the transmission coefficient T.

In the case that we can assume that $\frac{\pi}{\lambda}\Delta nd < \frac{\pi}{2}$, implying that $d < \frac{\lambda}{2\Delta n}$,

then there is only one solution, d, to Eq (1) :

80

$$d = \frac{\lambda}{\pi\Delta n} arctan\left(\sqrt{\frac{I_{LR}}{I_{LL}}}\right) \tag{2}$$

Therefore the thickness can be estimated by grabbing two images of a thin calcite crystals, taken one through a right circular polarizer (I_{LR}) and a second through a left circular polarizer (I_{LL}). I_{LL} has a dark background and calcite crystals appear lighter. I_{LR} has a light background and calcite particles appear darker. They are negative images of each other (Fig. 1a). The ratio $\frac{I_{LR}}{I_{LL}}$ increases with thickness (Fig. 1b). Applying Equation 2 to those two images gives the thickness and this depends on the

85 wavelength (λ) of the light used and the birefringence of calcite ($\Delta n = 0.172$).

3 Material

The methodology presented here was developed on a Leica DM6000 microscope, with a x100 objective having a numerical aperture of 1.47, and a condenser lens having a 1.2 numerical aperture. Three circular polarizers made by Chroma Technology Corp. are integrated in the microscope. One right circular polarizer is positioned as analyzer. It consists of a linear polarizer

90 oriented at +90° placed below a quarter-wave plate oriented at +45° mounted in a Leica cube and placed in the upper automatic turret of the microscope. This is a convenient place when one wants to automatically remove this analyzer to use other filters. If this not necessarily the analyzer can be placed in its regular position.

One (and one) left (right) circular polarizer, LCP (RCP), made of a quarter-wave plate oriented at 45° (-45°) followed by a linear polarizer oriented at 0°. These two polarizers are used alternatively when taking images of the same crystal. LCP and

95 RCP are placed in the revolving filter chamber of the automated condenser block. For a manual use, a quarter-wave plate could be placed under a linear polarizer, and rotated manually from -45° (LCP) to 45° (RCP).

One of five monochromatic bandpass filters centered at 435, 460, 560, 655, and 700 nm (AT435/20X, AT460/50M, ZET561/10X, AT655/30M and ET700/50M; all from Chroma Technology Corp.) is positioned in the light trajectory after the light bulb. The 561 nm filter is used in routine work because of its versatility (see below). The other filters are used to test the

100 method and in special occasions when study of relatively thick calcite particles in the range of 1.4-1.9 µm in the case of 700 nm; or for detail measurements of thin particles in the range of 0.2-0.4 nm for the 435 nm filter.

Two black and white numerical cameras are set up. A SpotFlex from Diagnostic Instrument, with a CCD image sensor of 2048x2048 pixels that are 7.4 µm large. It is a 14-bit camera (16383 grey levels in depth). And an Orca Flash 4.0 V2 from Hamamatsu, with a CMOS image sensor of 2048x2048 pixels that are 6.3 µm wide. It is a 16-bit camera (65548 grey levels

105 in depth). The tests of this method presented in results have been made with (i) surface sediment retrieved in the Southern Pacific and spread onto a slide, and (ii) calcium carbonate crystals precipitated onto a slide.

4. Results

To test the quality of the thickness estimations with the BCP method, the same field of view has been studied in different light conditions (lightness, opening, and wavelength) and with different cameras. In each condition, the two images I_{LL} and I_{LR} are

110 captured and used to compute the thickness d, with Equation 2. In some cases, in order to illustrate d, an image frame d_i in 8-bits, was computed using the following equation:

$$d_i = 256 \frac{d}{d_{max}} \quad (3)$$

where d_{max} represent the maximum measurable thickness at a given wavelength. It is calculated using the following equation:

$$d_{max} = \frac{\lambda}{\pi \Delta n} \cdot \frac{\pi}{2}$$

115 For calcite crystals, d_{max} ranges between 1.17 µm at 405 nm and 2.03 µm at 700 nm.

4.1 Lightness

The same field of view was captured at different time exposures with the SpotFlex camera. Exposure time is the simplest way to change the lightness of an image. Figure 2 shows that the fields of view captured at short exposure time (e.g., 5 ms) are extremely dark and conversely those captured at long exposure time (e.g., 320 ms) are light with many saturated areas

120 (maximum Grey Level (GL) values). Except for those two extreme expositions (i.e., 5 ms and 320 ms) the GL values are identical. In Fig. 3 the histograms of I_{LL}, I_{LR} and d are shown. At 320 ms the images are too light, and many areas are saturated both in I_{LL} and I_{LR} and thus have the same GL values. Knowing that the solution of Equation 2 is 0.81 µm when $I_{LL}=I_{LR}$ and λ = 561 nm, a spurious density peak appears in the histograms at a thickness of 0.81 µm with an exposure time longer than 320 ms (Fig. 3). In areas where I_{LL} is saturated but not I_{LR}, the estimations are shifted toward thicker values, explaining the

125 thicker density pick found at 0.7 µm in the histogram of 320 ms (Fig. 3). The image background, materialized in the histograms by the first peak, is around 0.1 µm for all exposures but is shifted toward higher thickness up to 0.2 µm at 320 ms.

At 5 ms, the images are too dark to provide correct estimation of the background level (Fig. 3) which, in turn, increases noise in the results. Therefore, in order to get correct thickness values, it is important to avoid too low or too high lightness. Between those extremes light conditions, the estimates of thicknesses are independent from the lightness. To get the maximum depth

130 details, it is suggested to use the maximum light before saturation in I_{LL}, providing the highest range of grey levels in both images. In the example given in Fig. 2, this maximum detail would be achieved between 80 ms and 160 ms.

The optical setting used in this experiment was not able to produce the darkest values (close to 1) and lightest value (equivalent to 255 in 8-bit). The reason why those extreme values are not reached is largely due to the imperfections of the circular polarizers that are composed of two layers. Those imperfections are amplified at the extremes of the light ranges because of

135 the sigmoid shape of the thickness function (Fig. 1). In practice, the ratio I_{LR} / I_{LL} is reached in the flattest part of the sigmoids (Fig. 1b), for example between 0.10 µm and 1.41 µm with 561 nm light wavelength. In consequence, the thickness measured in absence of particle was 0.10 µm at 561 nm when it should be 0. Also, the maximum measurable thickness is lower than the maximum theoretical thickness: using a wavelength of 561 nm, we obtain a maximum of 1.45 µm of thickness instead 1.62 µm (Fig. 3).

140 4.2 Aperture

The illumination tuning of the microscope is also important. The range of measurable thickness is largest when the condenser is focused and centered following the Köhler illumination (Köhler, 1894). More the field diaphragm is close, wider is the range of measurable thickness (Fig. 4). Hence, both diaphragms (i.e., field and aperture) should be closed at their maximum in order to maximize the range of measurable thickness.

4.3   Camera Type

The two tested camera types (CMOS vs CCD; 14-bit vs 16-bit; different brand) produced the same measure. The same view field was captured with two different camera type without measurable difference between the two resulting thickness images (Fig. 5).

The theoretical maximum measurable thickness (d_{cmax}) depends on the number of grey levels (nGL) achieved by the camera:

$$d_{cmax} = \frac{\lambda}{\pi \Delta n} arctan \left(\sqrt{\frac{nGL}{1}} \right)$$

At $\lambda = 561 nm$, d_{cmax} is 1.565 µm with an 8-bit camera, 1.622 µm with a 14-bit camera and 1.626 µm with a 16-bit camera. These d_{cmax} are far above the maximum measurable thickness of 1.45 µm described in section 5.a. However, the low depth resolution of an 8-bit camera should further limits the range of measurable thickness, although this was not tested here. Hence, both 14-bit and 16-bit can be used but we don't recommend to use 8-bit camera.

4.4   Accuracy and Precision

It is extremely difficult to estimate the measurement error in the present case because there is no standard material for thickness comparison in the range of few nanometers. The thickness of the wedge used to estimate the accuracy in González-Lemos et al. (2018) is measured at 250 nm intervals which is not enough in our case. Also, its measurements are based on a birefringence principle that is not strictly independent from our methodology. However, González-Lemos et al. (2018) clearly validate the accuracy of birefringence method at 250 nm. The measurement of coccoliths made by coherent X-ray diffraction (CXDI) at ESRF (Beuvier et al., 2019) require the use of silicon nitride (Si3N4) TEM windows influencing birefringence. Hence, those coccoliths cannot be used later as standard. However, in this study, coccoliths mass and size measurements from the same culture using both birefringence and CXDI provide a comparison on statistically similar results. The validity of the birefringence method is also demonstrated, although without giving a value to the accuracy. The use of cylindric rods such as rhabdoliths (Beaufort et al., 2014;Fuertes et al., 2014) is limited by the precision of the microscope used to produce the measurement of their diameter, around 0.2 µm in our microscope. The BCP method does not use any calibration, it is therefore theoretically absolute. It is accurate in the range given by the inflection points in Fig. 1.

We determine the precision of the BCP method at the five different wavelengths by using the two cameras on the same 7.74 µm transect of a *Pontosphaera japonica* (Fig. 6), producing 10 series of measurements. At the difference with Fig. 5, we voluntarily did not produce identical focus and use different wavelengths in order to produce generalized values. The root-mean-square error (RMSE) between two series is used to determine the precision of the method. When the wavelength are separated, the 5 RMSE range between 14 nm and 47 nm. The large RMSE values result from different focuses and/or red colors (635 nm and 700 nm). Best results were obtained at 561 nm and 435 nm with similar focus. When one series of measurements was compared to the average of all the other series, the RMSE = 32 nm. When it is limited to 435 nm to 561 nm, the RMSE = 12 nm. As we explain in detail in the next section, longer wavelengths in red lower the precision. This is an order

of magnitude smaller than the spatial optical resolution which ranges between 150 nm and 240 nm in the present microscopic setting at the 5 different wavelengths. The precision of the BCP method is expected to be smaller in many cases. For example, the RMSE in the transect of Fig. 5 is 5 nm. The difference of RMSE between Figs. 5 and 6 is related essentially to the focus that was well reproduced in Fig. 5. The estimated masses of P. japonica in Fig. 6, is ranging from 65.3 pg to 69.9 pg with a
180   standard deviation of 1.28 pg (N=10) and depends again, on the wavelength and the focus.

4.5   Wavelength and range of mesurable thickness

The comparisons of the same transects captured at different wavelengths along an image frame containing thick $CaCO_3$ particles emphasize the advantages and limits of each light wavelength. The range of thickness measurable at a given wavelength is presented in Fig. 7. In the transects, a plateau is reached at the maximum practical thickness (MPT) ; and when
185   the particle thickness is about 0.5 μm above the MPT, the thickness values decrease. It is not entirely clear why MPT is about 84% lower than the maximum measurable thickness (d_{max}). This difference has been described earlier (Bollmann, 2014). This discrepancy could be resulting from the quality of circular polarizers used. The circular polarizers are made with polaroid filters that are not perfect and are composed of two filters – a quarter-wave plate and a polarizer – creating some imperfections. As an example, linear polarizers exhibit generally larger range of grey levels with darker background than circular polarizers.
190   For the study coccoliths thicker than 1 μm like those of the Eocene, we recommend to use a light with long wavelengths (e.g., red at 700 nm). On the contrary, for the study of thin coccoliths such as most extant and Pleistocene species, we recommend to use shorter wavelengths (e.g., green or blue). Short wavelengths reached a MPT at lower thickness but offer higher precision in the measurement of the thickness and higher optical resolution permitting higher precision in the measurement of the area. The distal shield of Emiliania huxleyi coccoliths illustrate well an extreme measurement cases where the lower wavelength
195   has to be used to get a precise thickness and mass measurements. The distal shield of *E. huxleyi* is constructed with thin – ~100 nm – elements that do not touch each other (Fig. 8). The detection of those elements above the background is extremely difficult using wavelength at 700 nm but is possible using wavelength at 435 nm. In consequence, mass measurements are underestimated at 700 nm because the distal shield is not completely detected and producing a total area smaller than it is really (Table 1). Finally, this new method cannot give accurate results for calcareous nannofossils) thickness above 1.7 μm
200   like Cretaceous *Nannoconus* species. For such material, we recommend to be critical with results close to MPT and to use a color camera (Beaufort et al., 2014; González-Lemos et al., 2018) as in Fig. 7, although less precise than the BCP method related to some calibration issues (González-Lemos et al., 2018).

5   Conclusions

The alternative use of left and right circular polarization permits to measure the thickness of calcite crystals in a universal
205   manner without precise calibration of light. The BCP method has a great advantage from previous methods for which it is difficult to maintain stable light (i) in time (i.e., bulb aging, condenser vertical position,…) and (ii) in space since the field of

view may not be uniformly illuminated (i.e., low quality lens, uncentered condenser, ...). In all situations mentioned above, the previously published linear or circular polarizer methods will provide different thicknesses measurements whereas the BCP method described here will provide the same values. The choice of the wavelength of the light used for the measurements is specific to a targeted thickness. Thicker crystal will require longer wavelengths. Shorter wavelengths are recommended for precise measurement of thin crystals. In practice, upper and lower limits of measurements depend on the quality of polarizers and on the tuning of the microscope (Kohler illumination and close diaphragms). With our microscope, the practical range of measurements is 84% of the theoretical range. For example,at 561 nm, the lower measurable thickness is 0. 10 µm and the largest is 1.45 µm when theoretically the range should be 0 to 1.61 µm. It could be interesting to test if other type of circular polarizers such as mineral ones could provide larger practical ranges. The precision of the thickness measurements are an order of magnitude smaller – 0.012 µm to 0.030 µm – than that measurements of the length related to the resolution of an optical microscope that is approximatively 0.20 µm using natural light.

References

Beaufort, L.: Weight estimates of coccoliths using the optical properties (birefringence) of calcite, Micropaleontology, 51, 289-298, 10.2113/gsmicropal.51.4.289, 2005.

Beaufort, L., Barbarin, N., and Gally, Y.: Optical measurements to determine the thickness of calcite crystals and the mass of thin carbonate particles such as coccoliths, Nat. Protoc., 9, 633-642, 10.1038/nprot.2014.028, 2014.

Beuvier, T., Probert, I., Beaufort, L., Suchéras-Marx, B., Chushkin, Y., Zontone, F., and Gibaud, A.: X-ray nanotomography of coccolithophores reveals that coccolith mass and segment number correlate with grid size, Nat. Commun., 10, 751, 10.1038/s41467-019-08635-x, 2019.

Bollmann, J.: Technical Note: Weight approximation of coccoliths using a circular polarizer and interference colour derived retardation estimates – (The CPR Method), Biogeosciences, 11, 1899-1910, 10.5194/bg-11-1899-2014, 2014.

Fuertes, M. A., Flores, J. A., and Sierro, F. J.: The use of circularly polarized light for biometry, identification and estimation of mass of coccoliths, Mar. Micropaleontol., 113, 44-55, 10.1016/j.marmicro.2014.08.007, 2014.

González-Lemos, S., Guitián, J., Fuertes, M. Á., Flores, J. A., and Stoll, H. M.: Technical note: An empirical method for absolute calibration of coccolith thickness, Biogeosciences, 15, 1079-1091, 10.5194/bg-15-1079-2018, 2018.

Hassenkam, T., Johnsson, A., Bechgaard, K., and Stipp, S. L. S.: Tracking single coccolith dissolution with picogram resolution and implications for CO2 sequestration and ocean acidification, P. Natl. Acad. Sci. USA, 108, 8571-8576, 10.1073/pnas.1009447108, 2011.

Jones, R. C.: A new calculus for the treatment of optical systems – I. Description and discussion of the calculus, J. Opt. Soc. Am., 31, 488-493, 10.1364/JOSA.31.000488, 1941.

Köhler, A.: New method of illumination for photomicrographical purposes, J. Roy. Microsc. Soc., 14, 261-262, 1894.
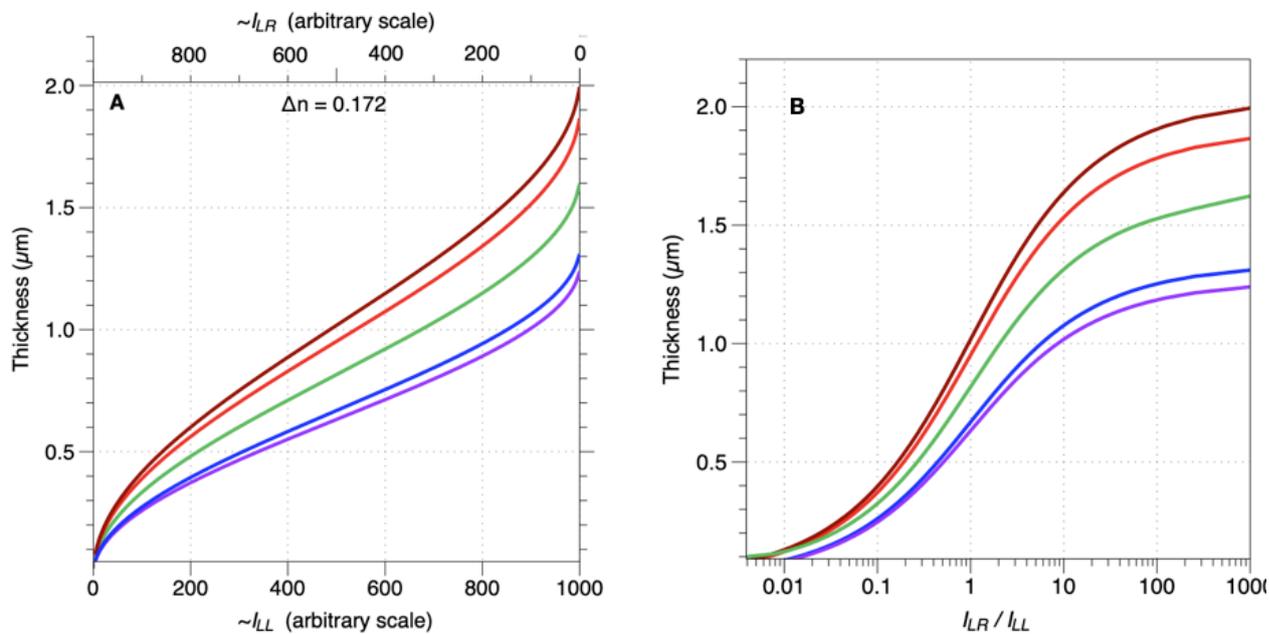
Figure 1: A. Light intensity (arbitrary scale from min=0 to max=1000) going through a left circular polarizer (I_{LL}) (top scale) or a right circular polarizer (I_{LR}) (bottom scale) associated with a left circular analyzer in relation to the thickness of calcite crystals (birefringence $\Delta n = 0.172$), under monochromatic light of wavelengths of 435 nm (indigo curve), 460 nm (blue curve), 561 nm (green curve), 665 nm (red curve) and 700 nm (brown curve). B. Light intensities ratio (I_{LR}/I_{LL}) under monochromatic light of the same wavelength as in A in relation to calcite crystals thickness.

240

245
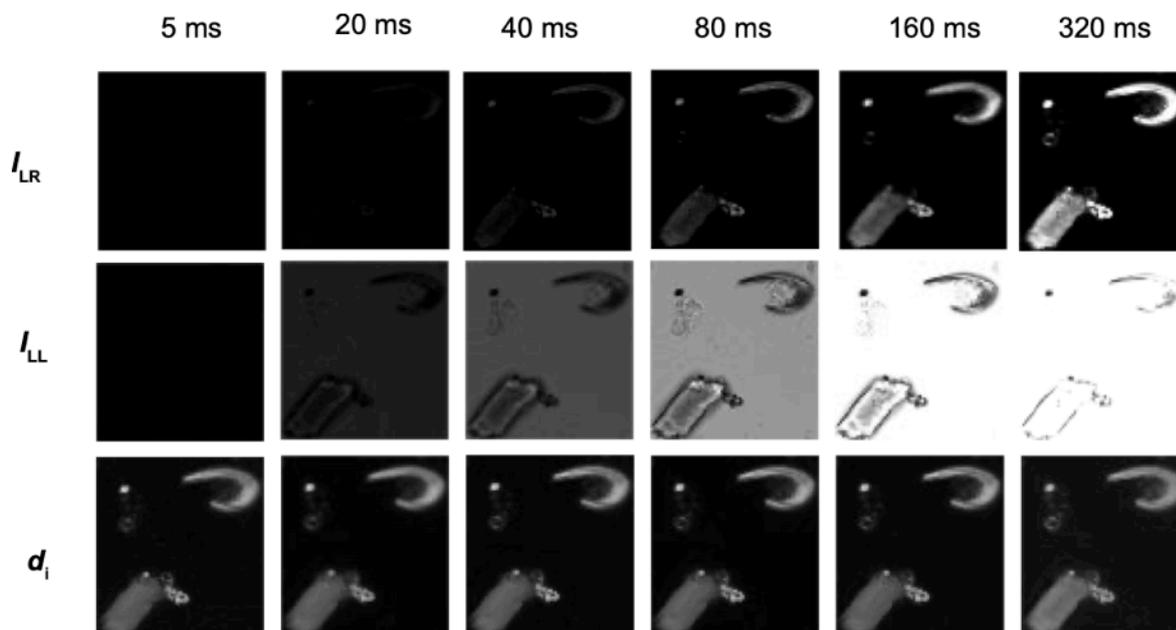
Figure 2: Crops of images captured at different times exposure (in columns; 5 ms, 20 ms, 40 ms, 80 ms, 160 ms, 320 ms) in right circular polarization (first row; I_{LR}), left circular polarization (second row; I_{LL}) and resulting thickness using Equations 2 and 3 with λ = 561 nm (third row; d_i). The resulting thickness images are very similar in the range of time exposure.
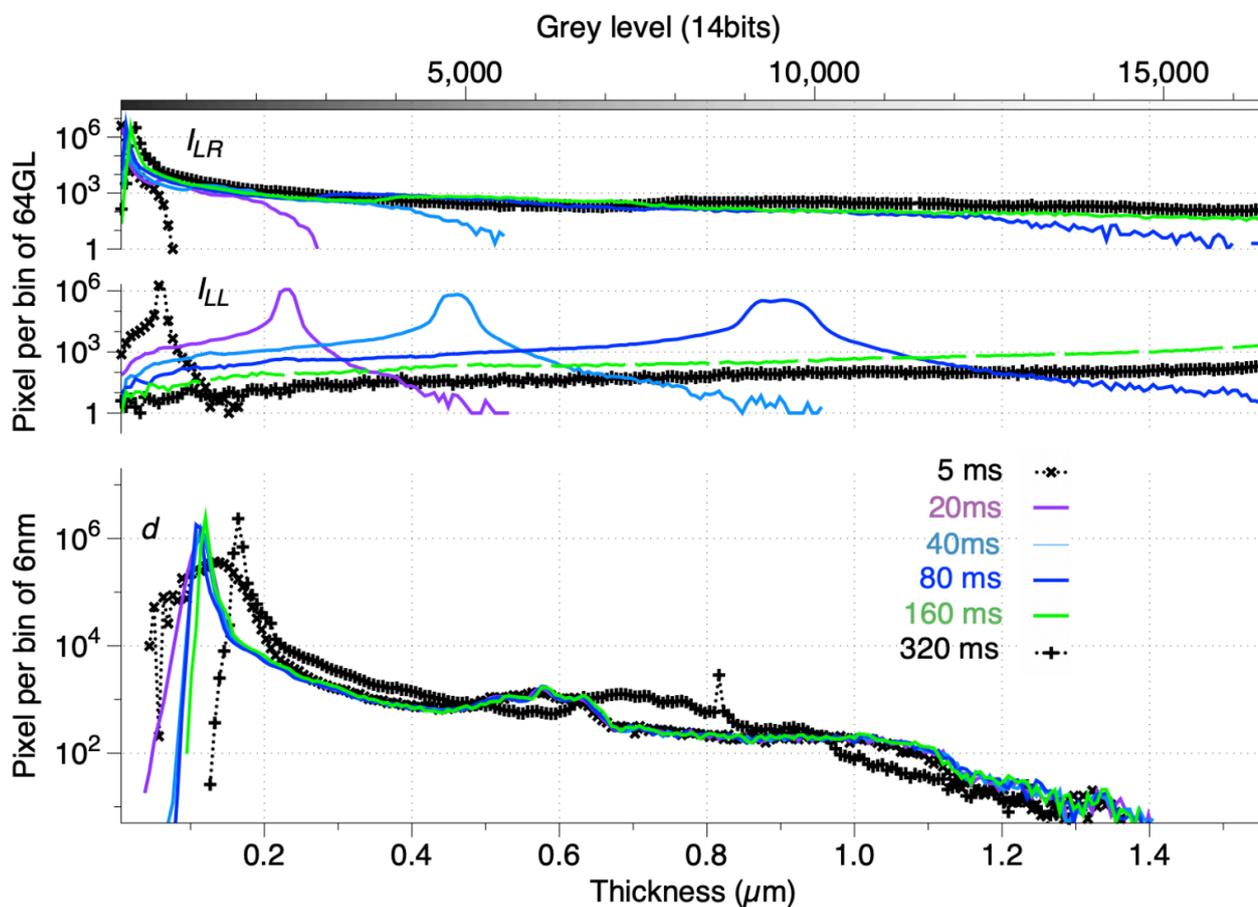
Figure 3: Histograms (bins of 64 grey levels (top) and 6 nm (bottom)) of the same field of view as in Fig. 2 , captured with green monochromatic light λ = 561 nm in right circular polarization (top), left circular polarization (middle), and the resulting thickness using Equation 2 (bottom) at different exposure times (black with plus signs: 5 ms, purple: 20 ms, light blue: 40 ms, blue: 80 ms,
255 green: 160 ms and black with crosses: 320 ms).
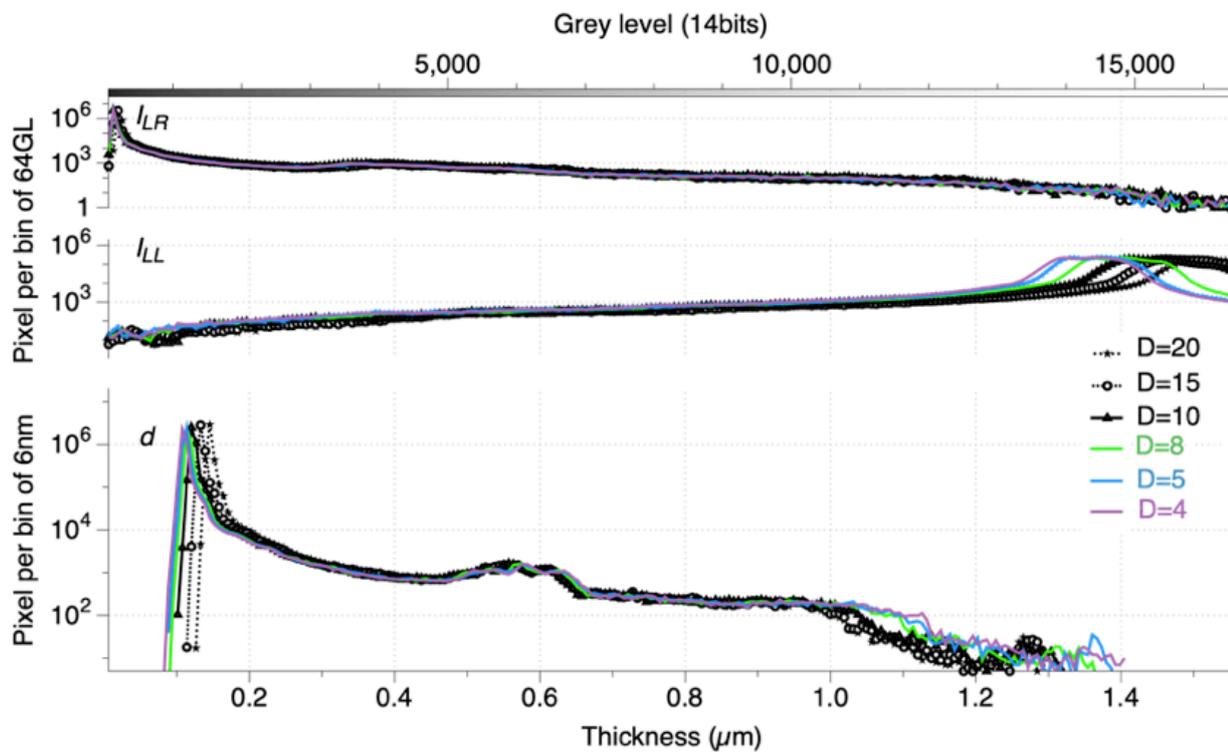
Figure 4: Histograms (bins of 64 grey levels (top) and 6 nm (bottom)) of the same field of view as in Fig. 2 , captured with green monochromatic light λ = 561 nm in right circular polarization (top), left circular polarization (middle), and the resulting thickness using Equation 2 (bottom) at different openings (Leica DM6000B scale ranging from 1 (closed) to 20 (open)) of the field diaphragm

260 (black with stars: 20, black with circles: 15, black with squares: 10, green: 8, blue: 5 and purple: 4).
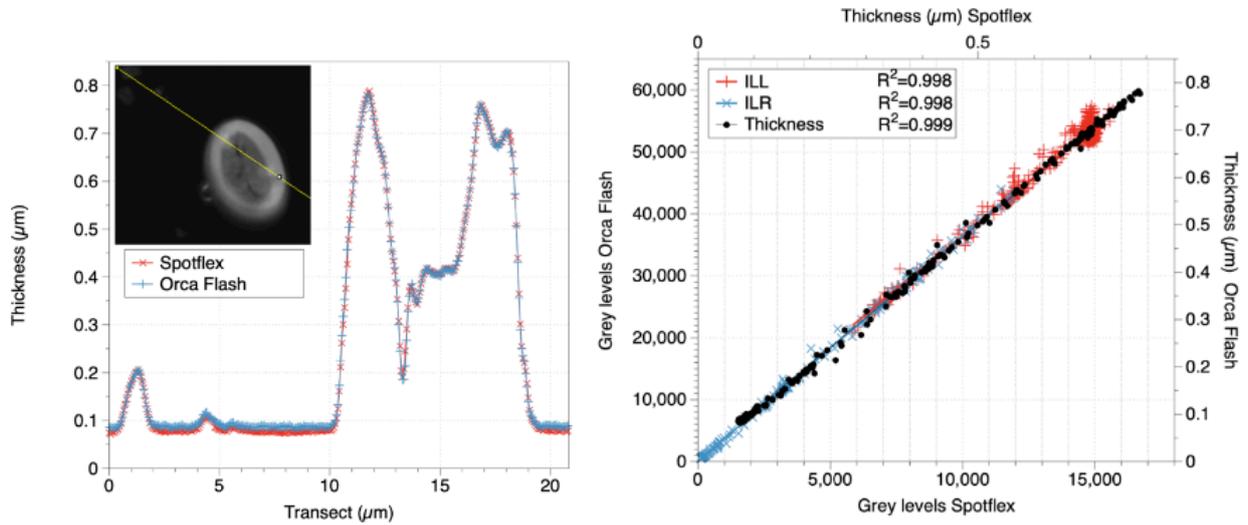
Figure 5: A: Thickness along a transect (yellow line in the inset) measured with the Spotflex (red line with crosses) and the Orca Flash cameras (blue line with plus signs). B: Relation between I_{LL} (red), I_{LR} (blue) and thickness (black) measurements made by the two cameras along the same transect.
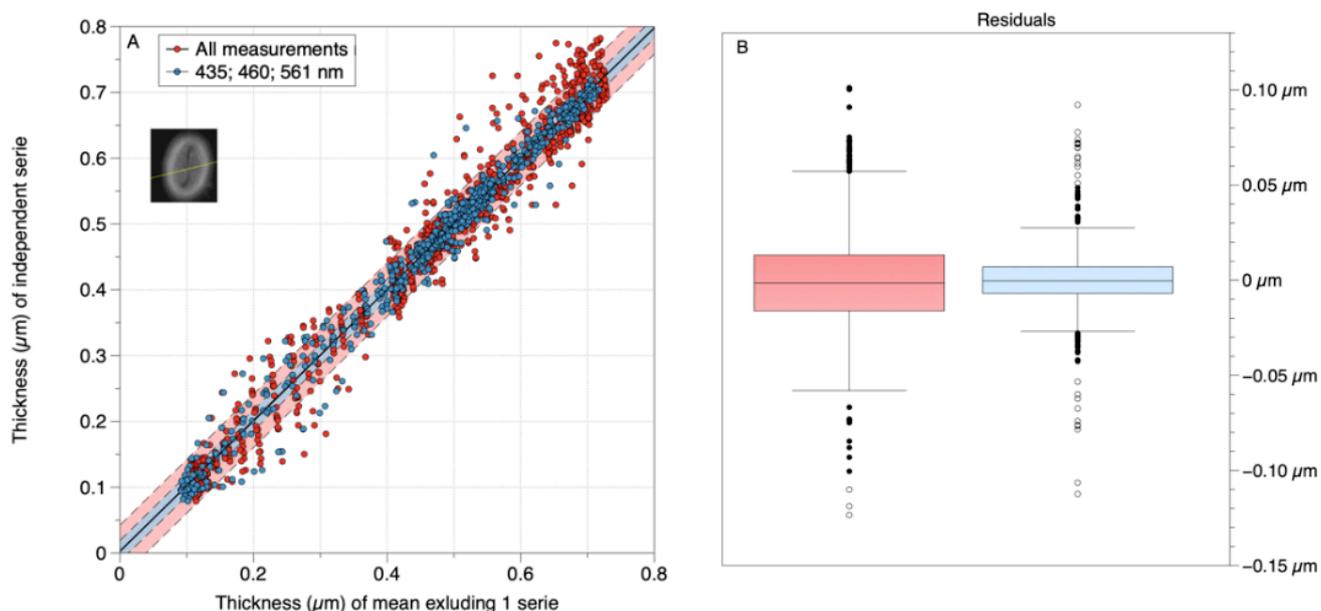
Figure 6: Precision of measurements made on the same 7.74 μm transect (yellow line in the inset) across a *Pontosphaera japonica* (inset) with 2 cameras and at 5 or 3 wavelengths, producing respectively 10 or 6 series of 129 points. Red: all wavelengths ($r^2 = 0.996$; RMSE = 0.032 μm); Blue: 435, 460 and 561 nm ($r^2 = 0.994$; RMSE = 0.012 μm). A. Relation between measure of a thickness series compared with the average of all the others. the average thickness of 9 (or 5) series along a transect and the thickness in the independent (not included in the average) series. The colored area represents the 80% prediction bounds. B. Whisker plots of the residual, bars represent the interquartile range, box represents the range between the 1st and 3rd quartiles. Standard deviation = 0.032 (left in red) and = 0.019 (right in blue).

Biogeosciences
10.5194/bg-2020-28
2020-02-04
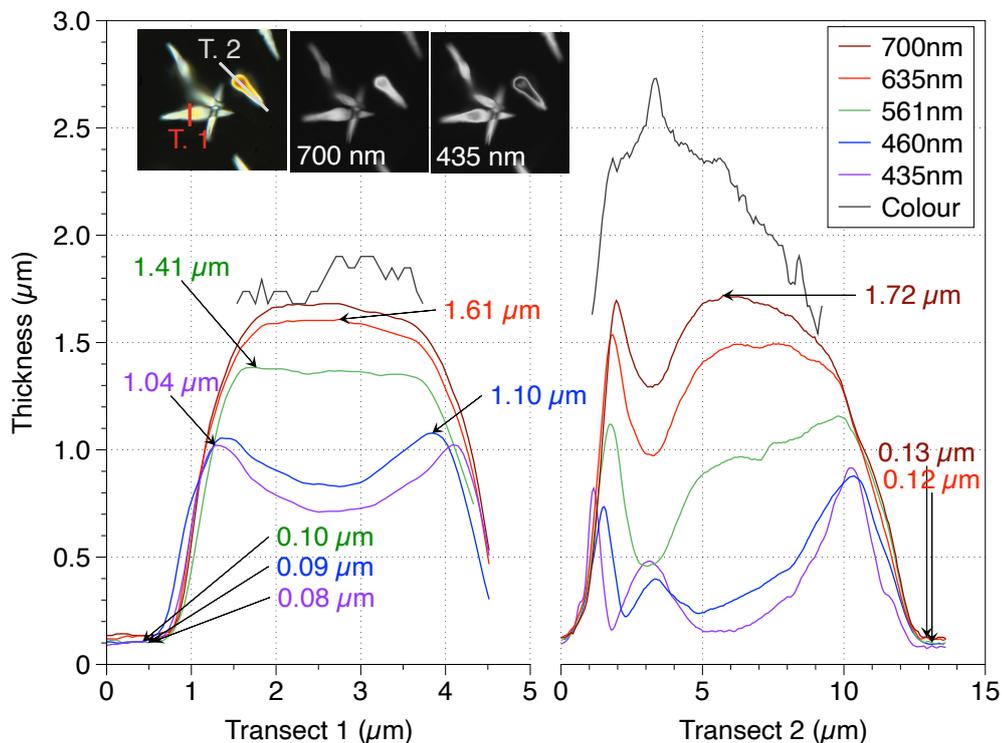
Figure 7: Thickness measurements made along two transects (T.1 in red and T.2 in white lines in the left inset) of CaCO₃ crystals at 5 wavelengths (brown lines: 700 nm; red lines: 635 nm; green lines: 561 nm; blue lines: 460 nm; indigo lines: 435 nm) and with a color camera (black lines; using the Hue values transfer function for thickness from Beaufort et al. (2014) – this latter method allows measurement up to thickness of 4.5 µm after a complex calibration). The 3 insets represent the images taken with a color camera (Spotflex) (left), a black and white camera (Spotflex) at 700 nm (center) and the same camera at 435 nm (right). The maximum and minimum measurements for each wavelength are indicated with an arrow.

280

285
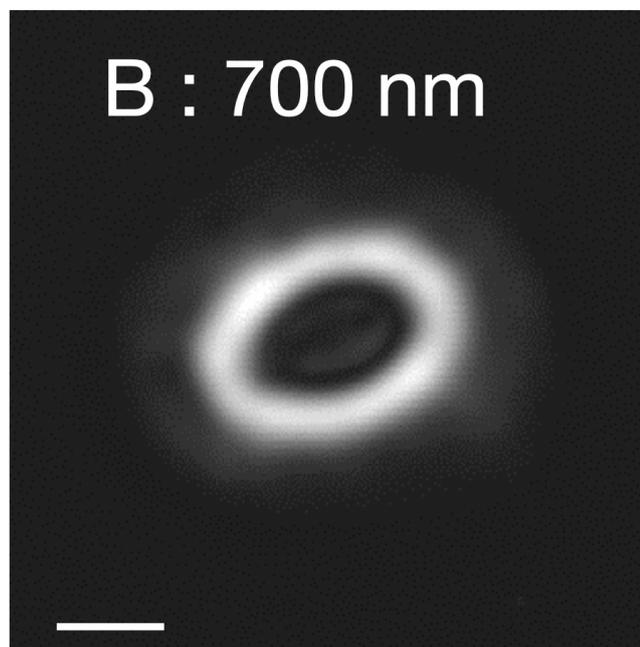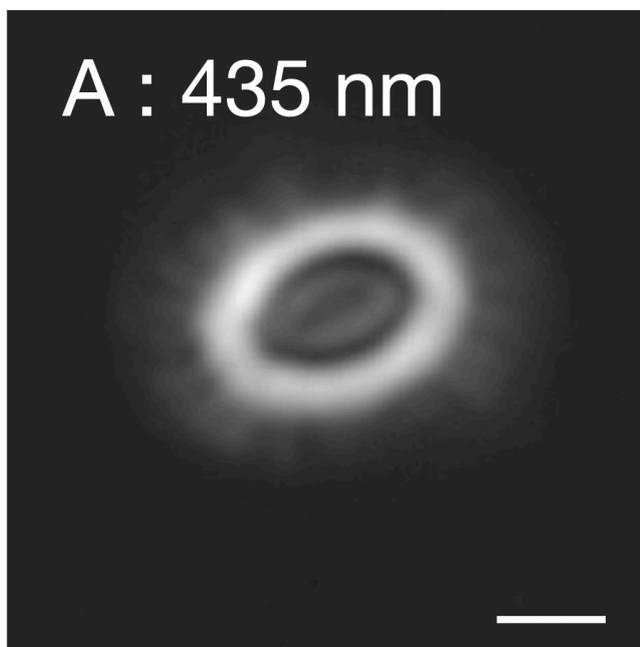
Figure 8: Images of a coccolith of *Emiliania huxleyi* captured at wavelengths 435 nm (A) and 700 nm (B). White bars are 1 μm long. Lightness has been adapted to enhance the contrast between background and elements from the distal shield.

290

Lambda nm	Optical spatial resolution (nm)	d_max (μm)	Mass (pg)	Area (μm2)
435	148	1.26	4.43	7.97
460	156	1.34	4.23	7.94
561	191	1.63	4.30	7.94
635	223	1.90	3.97	7.12
700	238	2.03	3.96	6.53

Table 1: Parameters and measurements of the coccoliths of *Emiliania huxleyi* presented in Fig.7.